ACCSCIENCE PUBLISHING

International Journal of Bioprinting

RESEARCH ARTICLE

Biomimetically hierarchical scaffolds drive critical-sized osteochondral tissue regeneration

Supplementary File

1. Materials and methods

1.1. Materials

Polycaprolactone (PCL) filaments (diameter 1.75 mm) was purchased from Esun Co. (Shenzhen, China). Dopamine hydrochloride (DOPA-HCl; Mw 189.64 g/mol), (3-glycidyloxypropyl)trimethoxysilane (GPTMS; Mw 236.34 g/mol), sodium hydroxide (Mw 40 g/mol), and 2,2,2-trifluoroethanol (TFE; Mw 100.04 g/mol) were purchased from Rhawn Co. (Shanghai, China). Bone morphogenic protein-2 (BMP-2) was purchased from Peprotech Co. (NJ, USA). Gelatin (Mw 40–50 kDa), isopropanol (99.99%, Mw 60.10 g/mol), ethanol (Mw 46.07), glutaraldehyde (25%, Mw 100.12 g/mol), tris(hydroxymethyl)aminomethane (Mw = 121.14 g/mol), phosphate-buffer saline (PBS, tablet, pH 7.2–7.4), sodium chloride (NaCl; Mw 58.44 g/mol), potassium chloride (KCl, Mw 74.55 g/mol), sodium bicarbonate ($NaHCO_3$; Mw 84.01 g/mol), calcium chloride dihydrate ($CaCl_2{\cdot}2H_2O$, Mw 147.01 g/mol), magnesium chloride hexahydrate ($MgCl_2{\cdot}6H_2O$; Mw 203.30 g/mol), sodium phosphate monobasic monohydrate ($NaH_2PO_4{\cdot}H_2O$; Mw 137.99 g/mol), and p-nitrophenyl phosphate (p-NPP; tablet) were purchased from Sigma-Aldrich Co. (MO, USA). Hydrochloric acid (HCl; 37%, Mw 36.46 g/mol) was purchased from Sinopharm reagent Co. (Shanghai, China). Dulbecco's Modified Eagle's Medium (DMEM), fetal bovine serum, and penicillin-streptomycin were purchased from Gibco-BRL, Life Technologies Co. (NY, USA). Alkaline phosphatase (ALP) kit was purchased from Beyotime Biotechnology Co. (Shanghai, China). BCA (bicinchoninic acid) protein assay kit was purchased from Thermo Fisher Scientific Co. (MA, USA). Osteocalcin (OC) enzyme-linked immunosorbent assay kit was purchased from Sino Biological Co. (Beijing, China). CCK-8 assay kit was purchased from Dojindo Molecular Technologies Co. (MD, USA). Propidium iodide and calcein-AM were purchased from Beijing Solarbio Science & Technology Co. (Beijing, China). Radioimmunoprecipitation assay buffer (RIPA) was purchased from Bioteke Corporation Co. (Wuxi, China). Aqueous solutions were prepared with deionized water. All reagents were used without further purification.

1.2. Characterization

Analysis of pore size and fiber diameter was performed using Image Measurement Software (KLONK Image Measurement Light, Edition 11.2.0.0) based on field emission scanning electron microscopy (FE-SEM) micrographs.

1.3. 10 × simulated body fluid solution preparation

The 10× simulated body fluid (SBF) solution was prepared in accordance with the methodology outlined in a prior investigation.[1] In summary, the chemical constituents listed in Table S1 were dissolved in deionized water at room temperature. Subsequently, additional deionized water was introduced to the resultant solution, followed by adjustment of the pH to a range of 4.3–4.4. This stock solution was maintained at 4°C and fortified with 10 mM $NaHCO_3$ at each incubation interval during the assessment of bioactivity. Upon the addition of $NaHCO_3$, the pH of the solution was elevated to 6.5, rendering it suitable for conducting bioactivity assays.

1.4. Isolation of rat bone marrow mesenchymal stem cells

The animal experimentation protocols were approved by the Animal Care and Use Committee at the Fudan University Hospital Medical Center (code 2021-DS-Q-16), and the study was conducted in strict adherence to the ethical principles outlined by the National Institutes of Health (NIH) regarding the care and utilization of laboratory animals.

Four-week-old male Sprague–Dawley rats were procured from the Shanghai Lab Animal Research Center (Shanghai, China) and were maintained under standard housing conditions. Subsequent to euthanasia, the rats underwent sterilization with 70% ethanol for a

Table S1. Concentration of the reagent in a 10× SBF solution

Reagents	Amount (g/L)	Concentration (mM)
NaCl	58.443	1000
KCl	0.373	5
$CaCl_2 \cdot 2H_2O$	3.675	25
$MgCl_2 \cdot 6H_2O$	1.016	5
$NaH_2PO_4 \cdot H_2O$	0.250	3.62
$NaHCO_3$	0.084	10

duration of 15 min. The femur and tibia bones were then removed, following which bone marrow was harvested via centrifugation (Beckman Allegra X-15, Beckman Coulter Co., CA, USA) at 800 rpm for 10 min. The isolated cells were resuspended in DMEM supplemented with 10% v/v fetal bovine serum and 100 U/mL penicillin-streptomycin, and subsequently incubated at 37 ± 0.5 °C, with 5% CO_2 and 95% relative humidity. After 24 h, the culture medium was decanted along with non-adherent cells. This process of medium renewal was repeated every 3 days until 80% confluence of cells was attained.

1.5. Sterilization of scaffolds

Sterilization of scaffolds was carried out with ethylene oxide gas at a concentration of 600 ± 30 mg/L, a temperature of 54 ± 2 °C, and a humidity of 60 ± 10%.

2. Results and discussion

2.1. Pore size and strand diameter

Figure S1A shows digital photos of PC, PCD, and PCD cut scaffolds before FE-SEM imaging. The average pore size of PC and mono-phasic PCD scaffolds was 448 ± 21 and 429 ± 44 μm, respectively, whereas the strand width was increased from 356 ± 23 to 388 ± 40 μm, respectively (Figure S1B). These findings can be attributed to the polydopamine (PDA) deposited on the scaffold's surface. Electrospun PCL-gelatin fibers showed an average diameter of 2 ± 0.5 μm. We found that by directly immobilizing gelatin-BMP-2 on oxygen-plasma-modified fibers, the diameters of the fibers significantly increased to 3 ± 0.8 μm without altering uniformity (Figure S1C), which comes from fiber connections and a reduction in void spaces.

2.2. Chemical characterization

The chemical characterization of raw materials and composite scaffolds was conducted via Fourier transform infrared (FTIR) spectroscopy, as depicted in Figure S2. The distinct peaks at 2946 and 2865 cm^{-1} indicate the CH_2 stretching vibration in pure PCL. Additionally, peaks observed at 1721, 1294, and 1238 cm^{-1} are attributed to the stretching vibrations of C=O, C–C, and C–O–C (carbonyl and etheric functional groups), respectively.[2] In the case of PDA, a broad peak in the range of 3200–3500 cm^{-1}

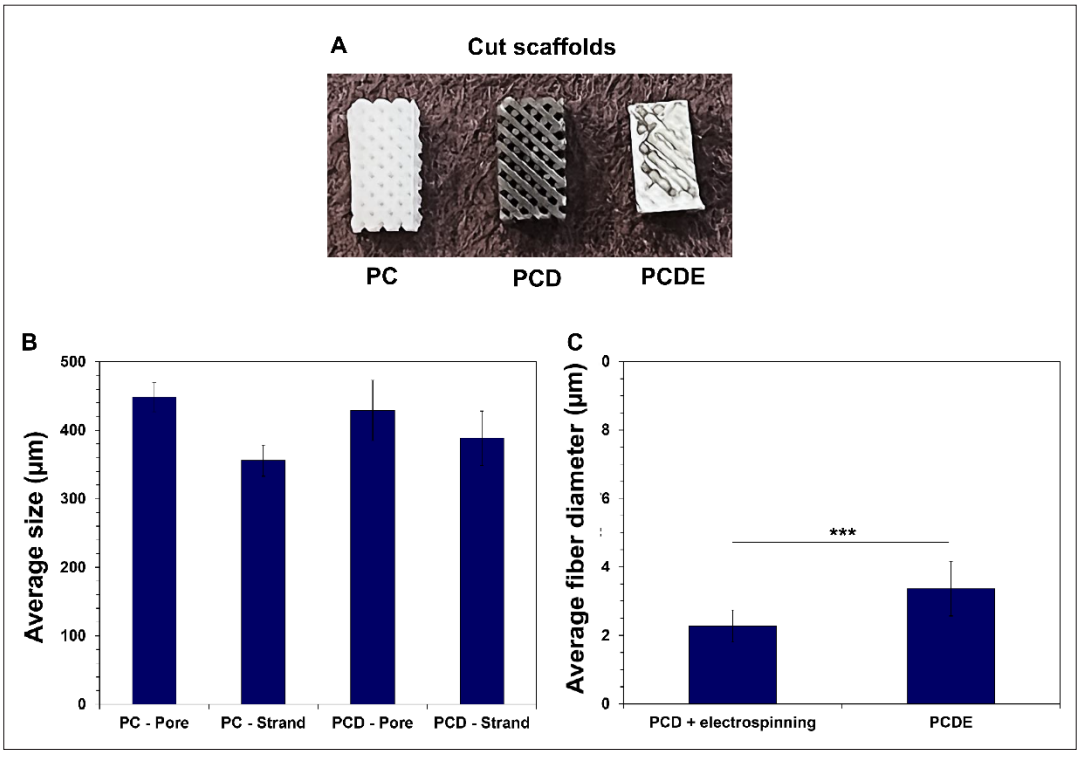

Figure S1. Macro and microstructural evaluation of the scaffolds. (A) Digital image of cut scaffolds before FE-SEM imaging. (B) Average pore and strand size in 3D-printed layers. (C) Average diameter of electrospun fibers. *** $p \leq 0.001$. Abbreviation: FE-SEM, Field emission scanning electron microscopy

corresponds to the stretching vibrations of phenolic O–H and N–H bonds associated with catechol groups.[3,4] An absorption peak at 1603 cm^{-1} identifies both the aromatic ring and the stretching and bending vibrations of the N–H group. Furthermore, N–H stretching vibrations of the amide group and C–O vibrations are observed at 1511 and 1119 cm^{-1}, respectively. The characteristic peaks at 1344 and 1285 cm^{-1} correspond to the bending and stretching vibrations of the phenolic C–O–H, respectively.[5] The spectrum of gelatin exhibits a broad peak in the range of 3200–3600 cm^{-1}, indicating N–H and O–H stretching vibrations. Additionally, the stretching vibrations of amide I and II are evident at 1633 and 1525 cm^{-1}, respectively.[6] Moreover, the peak at 1230 cm^{-1} is attributed to C–N and N–H couplings in amide III. For GPTMS, peaks at 2944 and 2812 cm^{-1} correspond to the CH_3 stretching vibration of methoxy groups. CH_2 vibrations in the glycidoxy and propyl chains are detected at 1195 and 1081 cm^{-1}, respectively. The presence of the epoxy group in the chemical composition of GPTMS is identified by peaks at 1254, 910, 859, and 436 cm^{-1}.[7]

The characteristic peaks observed in the PC constructs closely resemble those exhibited by pure PCL, indicating that the manufacturing process did not adversely influence the composition of the raw materials. Within the scope of this investigation, PC scaffolds were functionalized with a layer of PDA, which was synthesized through the spontaneous oxidation of dopamine hydrochloride in an alkaline milieu. This chemical transformation involves the oxidation of dopamine hydrochloride in an alkaline setting, leading to the formation of dopaminequinone. Subsequent deprotonation of the amine groups, coupled with a 1,4-Michael addition reaction, culminates in the generation of leucodopaminechrome. Oxidative conversion of leucodopaminechrome yields dopaminechrome, which undergoes rearrangement to produce 5,6-dihydroxyindole. The interaction between catechol groups and o-quinone within 5,6-dihydroxyindole precipitates the polymerization of PDA on the scaffold surface.[8] The polymerization process augments bonding forces, encompassing hydrogen bonds, bidentate chelation, coordination, as well as monodentate and bridged bidentate binding, thereby influencing the interaction between PDA and the substrate.[9] Consequently, the attachment of PDA to the surface is anticipated to be influenced by both covalent bonds and non-covalent interactions.[10] Concerning the covalent bonds formed during PDA coating on the PCL surface, chemical reactions such as nucleophilic addition or condensation reactions take place. In these reactions, the reactive groups on PDA (catechol moieties) engage with the functional groups along the PCL chains (–COO–), fostering cohesive crosslinking of marine adhesive proteins on PCL substrates.[11] Concurrently, non-covalent interactions, including hydrogen bonds, van der Waals forces, and

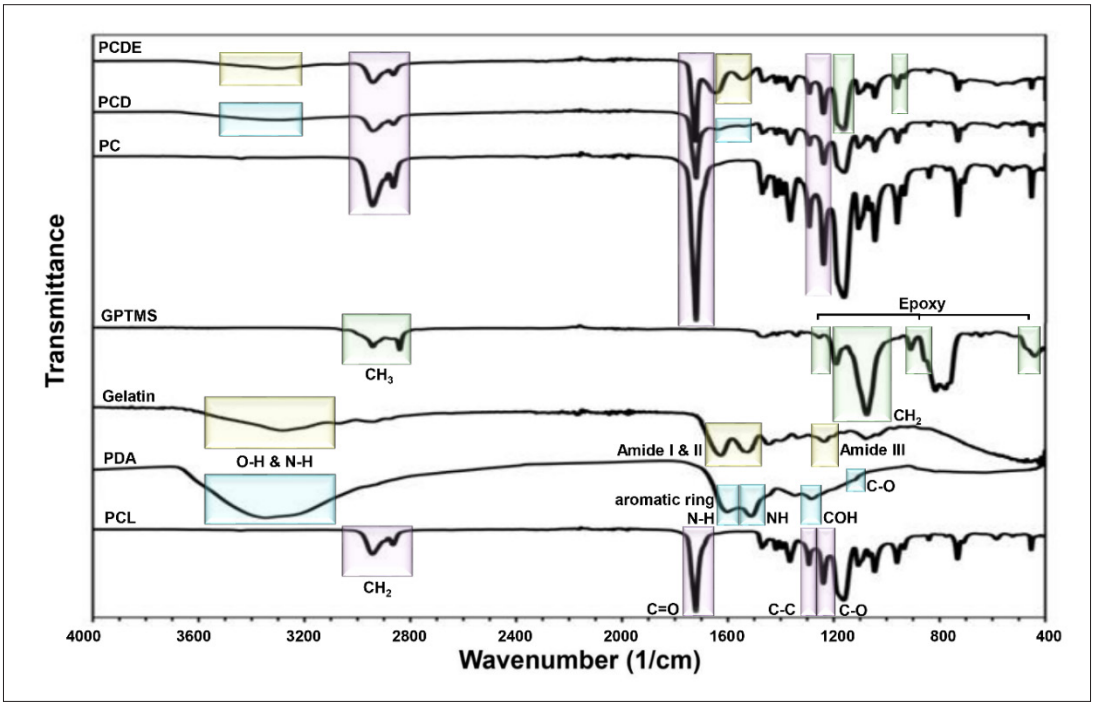

Figure S2. Chemical characterization of scaffolds: FTIR spectra of raw materials and composite structures. Abbreviation: FTIR, Fourier transform infrared spectroscopy; GPTMS, (3-Glycidyloxypropyl)trimethoxysilane; PCL, polycaprolactone; PDA, polydopamine.

hydrophobic interactions, contribute to the initial attachment of PDA to the PCL surface and play a pivotal role in the overall adhesion. Hydrogen bonding can occur between the hydroxyl groups of PDA's catechol moieties and carbonyl groups on the PCL. Besides, van der Waals forces, such as dipole–dipole interactions, can manifest between PDA and PCL, arising from the attraction between temporary dipoles (resulting from electron fluctuations) in one molecule and the induced dipoles in the neighboring molecules. Additionally, hydrophobic interactions may ensue between hydrophobic regions of PDA and hydrophobic segments of PCL, enhancing adherence and stability of the coating.[12,13] The polymerization of PDA on PC scaffolds is manifested by the emergence of peaks corresponding to PDA within the spectrum of PCD matrices. Despite the diminished intensity of C=O, C–O, and C–C bonds in the PCL chemical composition, a minor peak at 1630 cm^{-1} is attributable to the aromatic rings and N–H bonds present in PDA.[14] This observation may be attributed to the interaction between the carbonyl groups of PDA and the amine groups of PCL.[15]

In the multi-phasic PCDE scaffolds, the incorporation of crosslinked electrospun gelatin with GPTMS induced the emergence of discernible peaks associated with Si–O–Si and Si–OH functionalities, situated at 1160 and 950 cm^{-1}, respectively.[16] This occurrence stems from the interaction between amino groups within gelatin and the oxirane ring of GPTMS, thereby arresting the ring-opening reaction of epoxy groups. Subsequent events encompassed the hydration of trimethoxy moieties within the GPTMS framework, culminating in the generation of pendant silanol groups via acid-catalyzed transformations. Ultimately, a condensation reaction involving silanol groups engendered the establishment of Si–O–Si bonds and interchain covalent linkages, thereby effectuating the cross-linking of gelatin.[16] In the subsequent phase, multi-phasic scaffolds underwent immobilization with hydrogel-growth factor complexes post-oxygen plasma surface modification. The treatment with oxygen plasma induced the bombardment of surface chemical moieties with free radicals or ionized species, facilitating the generation of carbon radicals and transient peroxides. These peroxides, in turn, contributed to the formation of oxygen-containing functional groups, including carbonyl, carboxylic acid, and hydroxyl functionalities.[17] Notably, FTIR spectroscopy corroborated the disruption of CH linkages and the concomitant emergence of oxygen-containing functional groups, exemplified by the diminished intensity peak at approximately 2946 cm^{-1} and the augmented intensity peak at 1721 cm^{-1}. This phenomenon aligns with findings reported by Salapare et al.[18] Furthermore, the active radicals present on fiber surfaces promptly interacted with hydrogen entities within the gelatin-BMP-2 complex, thereby fostering enhanced immobilization of the subsequent layer. Additionally, hydrogen bonding between the oxygen-rich surface and gelatin-BMP-2, alongside the plausible formation of covalent bonds between methyl groups in the electrospun layer and hydroxyl groups in the gelatin-BMP-2 complex, fortified the integrity and stability of the immobilized layer. Analogous observations have been documented in extant literature.[19–22] Noteworthy increments in the intensity of hydroxyl groups at 3300 cm^{-1} corroborate these assertions.[23,24] The covalent immobilization of growth factors is anticipated to facilitate sustained stimulation of target cells while ensuring the maintenance of an efficacious dosage,[25] thereby potentiating the osteogenic differentiation of rat bone marrow mesenchymal stem cells (rBMSCs).

2.3. Bioactivity

In this investigation, the bioactivity of the scaffolds was evaluated employing a 10× SBF solution. The principal aim of the new SBF formulation, as distinguished from the conventional SBF solution, is to enhance the kinetics of carbonate hydroxyapatite formation characterized by nano-scale structures. This enhancement was achieved through the substitution of $K_2HPO_4{\cdot}3H_2O$ with $NaH_2PO_4{\cdot}H_2O$ and the modulation of bicarbonate (HCO_3^-) and chloride (Cl^-) ion concentrations, as delineated in Table S2.[26]

Table S2. Concentration of ions in 10× SBF solution compared to conventional SBF solution and human plasma[1]

Ion	Conventional SBF (mM)	10× SBF (mM)	Human plasma (mM)
Na^+	142.0	142.0	142.0
K^+	5.0	5.0	5.0
Mg^{2+}	1.5	1.5	1.5
Ca^{2+}	2.5	2.5	2.5
Cl^-	147.0	125.0	103.0
HCO_3^-	4.2	27.0	27.0
HPO_4^{2-}	1.0	1.0	1.0
SO_4^{2-}	0.5	0.5	0.5

Abbreviation: SBF, simulated body fluid.

References

1. Ghorbani F, Zamanian A, Behnamghader A, Daliri-Joupari M. Bone-like hydroxyapatite mineralization on the bio-inspired PDA nanoparticles using microwave irradiation. *Surf Interfaces*. 2019;15:38-42. doi: 10.1016/j.surfin.2019.01.007
2. Xiang P, Wang SS, He M, et al. The in vitro and in vivo biocompatibility evaluation of electrospun recombinant spider silk protein/PCL/gelatin for small caliber vascular tissue engineering scaffolds. *Colloids Surf B Biointerfaces*. 2018;163:19-28. doi: 10.1016/j.colsurfb.2017.12.020
3. Nishizawa N, Kawamura A, Kohri M, Nakamura Y, Fujii S. Polydopamine particle as a particulate emulsifier. *Polymers (Basel)*. 2016;8:62-77. doi: 10.3390/polym8030062
4. Luo H, Gu C, Zheng W, Dai F, Wang X, Zheng Z. Facile synthesis of novel size-controlled antibacterial hybrid spheres using silver nanoparticles loaded with poly-dopamine spheres. *RSC Adv*. 2015;5:13470-13477. doi: 10.1039/C4RA16469E
5. Fu J, Chen Z, Wang M, et al. Adsorption of methylene blue by a high-efficiency adsorbent (polydopamine microspheres): kinetics, isotherm, thermodynamics and mechanism analysis. *Chem Eng J*. 2015;259:53-61. doi: 10.1016/j.cej.2014.07.101
6. Ghorbani F, Zamanian A, Nojehdehian H. Effects of pore orientation on in-vitro properties of retinoic acid-loaded PLGA/gelatin scaffolds for artificial peripheral nerve application. *Mater Sci Eng C*. 2017;77:159-172. doi: 10.1016/j.msec.2017.03.175
7. Šapić IM, Bistričić L, Volovšek V, Dananić V, Furić K. DFT study of molecular structure and vibrations of 3-glycidoxypropyltrimethoxysilane. Spectrochim. *Acta - A Mol Biomol Spectrosc*. 2009;72:833-840. doi: 10.1016/j.saa.2008.11.032
8. Ghorbani F, Zamanian A, Behnamghader A, Joupari MD. A facile method to synthesize mussel-inspired polydopamine nanospheres as an active template for in situ formation of biomimetic hydroxyapatite. *Mater Sci Eng C*. 2019; 94:729-739. doi: 10.1016/j.msec.2018.10.010
9. Nielsen SR, Besenbacher F, Chen M. Mussel inspired surface functionalization of electrospun nanofibers for bio-applications. *Phys Chem Chem Phys*. 2013;15:17029. doi: 10.1039/c3cp52651h
10. Alfieri ML, Weil T, Ng DYW, Ball V. Polydopamine at biological interfaces. *Adv Colloid Interface Sci*. 2022;305:102689. doi: 10.1016/j.cis.2022.102689
11. Lee H, Scherer NF, Messersmith PB. Single-molecule mechanics of mussel adhesion. *Proc Natl Acad Sci U S A*. 2006;103:12999-13003. doi: 10.1073/pnas.0605552103
12. Ding YH, Floren M, Tan W. Mussel-inspired polydopamine for bio-surface functionalization. *Biosurf Biotribol*. 2016;2:121-136. doi: 10.1016/j.bsbt.2016.11.001.
13. Iqbal Z, Lai EPC, Avis TJ. Antimicrobial effect of polydopamine coating on Escherichia coli. *J Mater Chem*. 2012;22:21608. doi: 10.1039/c2jm34825j.
14. Jo S, Kang SM, Park SA, Kim WD, Kwak J, Lee H. Enhanced adhesion of preosteoblasts inside 3D PCL scaffolds by polydopamine coating and mineralization. *Macromol Biosci*. 13;2013:1389-1395. doi: 10.1002/mabi.201300203.
15. Ghorbani F, Zamanian A, Aidun A. Bioinspired polydopamine coating-assisted electrospun polyurethane-graphene oxide nanofibers for bone tissue engineering application. *J Appl Polym Sci*. 2019;136: 47656. doi: 10.1002/app.47656
16. Tonda-Turo C, Gentile P, Saracino S, et al. Comparative analysis of gelatin scaffolds crosslinked by genipin and silane coupling agent. *Int J Biol Macromol*. 2011;49:700-706. doi: 10.1016/j.ijbiomac.2011.07.002
17. Park J-M, Kim D-S, Kim S-R. Improvement of interfacial adhesion and nondestructive damage evaluation for plasma-treated PBO and Kevlar fibers/epoxy composites using micromechanical techniques and surface wettability. *J Colloid Interface Sci*. 2003;264:431-445. doi: 10.1016/S0021-9797(03)00419-3
18. Salapare HS, Tiquio MGJP, Ramos HJ. Superhydrophilic properties of plasma-treated Posidonia oceanica. *Appl Surf Sci*. 2013;273:444-447. doi: 10.1016/j.apsusc.2013.02.060
19. Kim YJ, Kang IK, Huh MW, Yoon SC. Surface characterization and in vitro blood compatibility of poly(ethylene terephthalate) immobilized with insulin and/or heparin using plasma glow discharge. *Biomaterials*. 2000;21:121-130. doi: 10.1016/S0142-9612(99)00137-4
20. Kang I-K, Kwon I-K, Lee YM, Sung YK. Preparation and surface characterization of functional group-grafted and hepk&-immobilized polyurethanes by plasma glow discharge. *Biomaterials*. 1996;17:841-847. doi: 10.1016/0142-9612(96)81422-0
21. Yoshinyari M, Hakawa T, Matsuzaka K, et al. Oxygen plasma surface modification enhances immobilization of simvastatin acid. *Biomed Res*. 2006;27:29-36. doi: 10.2220/biomedres.27.29

22. Adipurnama I, Yang M-C, Ciach T, Butruk-Raszeja B. Surface modification and endothelialization of polyurethane for vascular tissue engineering applications: a review. *Biomater Sci*. 2017;5:22-37. doi: 10.1039/C6BM00618C

23. Li X, Jiang Y, Wang F, *et al*. Preparation of polyurethane/polyvinyl alcohol hydrogel and its performance enhancement via compositing with silver particles. *RSC Adv*. 2017;7:46480-46485. doi: 10.1039/c7ra08845k

24. Solouk A, Cousins BG, Mirzadeh H, Seifalian AM. Application of plasma surface modification techniques to improve hemocompatibility of vascular grafts: a review. *Biotechnol Appl Biochem*. 2011;58:311-327. doi: 10.1002/bab.50

25. Pohl TLM, Schwab EH, Cavalcanti-Adam EA. Covalent binding of BMP-2 on surfaces using a self-assembled monolayer approach. *J Vis Exp*. 2013;(78):50842. doi: 10.3791/50842

26. Ghorbani F, Zamanian A, Behnamghader A, Joupari MD. Microwave-induced rapid formation of biomimetic hydroxyapatite coating on gelatin-siloxane hybrid microspheres in 10X-SBF solution. 2018;18(3):247-255. doi: 10.1515/epoly-2017-0196